ISSN 1063-7729, Astronomy Reports, 2006, Vol. 50, No. 10, pp. 842–850. © Pleiades Publishing, Inc., 2006.
Original Russian Text © A.I. Podgorny, I.M. Podgorny, 2006, published in Astronomicheskiĭ Zhurnal, 2006, Vol. 83, No. 10, pp. 940–949.

A Model of a Solar Flare: Comparisons with Observations of High-Energy Processes

A. I. Podgorny[1] and I. M. Podgorny[2]

[1] *Lebedev Institute of Physics, Russian Academy of Sciences, Leninskiĭ pr. 53, Moscow, 117924 Russia*
[2] *Institute of Astronomy, Russian Academy of Sciences, Pyatnitskaya ul. 48, Moscow, 109017 Russia*

Received December 5, 2005; in final form, April 14, 2006

Abstract—New data for the energy and location of the hard-emission centers of a solar flare agree with an electrodynamic model of a solar flare based on the idea of the accumulation of free magnetic energy in the field of a current sheet. Three-dimensional MHD simulations are used to show that the energy stored in the preflare magnetic field of the current sheet is sufficient for the development of a flare and a coronal mass ejection. The flare and coronal mass ejection result from the explosive decay of the current sheet. The position of the brightness-temperature maximum of the radio emission during the flare coincides with the maximum of the current in the current sheet. The exponential spectrum of relativistic protons generated during the flare is consistent with acceleration by the electric field during the current-sheet decay.

PACS numbers : 96.60.qe, 96.60.ph
DOI: 10.1134/S106377290610009X

1. INTRODUCTION

Solar flares and coronal mass ejections (CMEs) are the most violent manifestations of solar activity. The energy of a flare is released in the corona over an active region [1], and CMEs are, likewise, accelerated in the corona [2]. The energy released during major flares and the accompanying CMEs can reach about 10^{33} erg. The only source of this energy in the solar corona is so-called free magnetic energy, which can be accumulated in the magnetic fields of current systems over an active region and released rapidly during a flare in the form of heat, the kinetic energy of plasma streams, electromagnetic radiation, and accelerated charged particles. A necessary condition for an explosive flare process is that there be a high energy density stored in the current fields, $B_c^2/8\pi$, compared to the plasma-energy density nkT; i.e., $\beta = 8\pi nkT/B_c^2 \ll 1$. Here, B_c is the magnetic field of the currents in the plasma, n is the number density of particles, T is the temperature, and k is Boltzmann's constant. Such conditions can be realized in the corona as current circuits develop over an active region. We emphasized that, here, β is not a dimensionless parameter that can be calculated based on the potential magnetic field of the active region. The potential magnetic field is only responsible for creating the conditions for the development of a current, whose magnetic field can become an accumulator of free magnetic energy. Thus, a model of the flare must include a mechanism for the accumulation of the energy of the current magnetic fields and the explosive conversion of this energy into other forms; i.e., a mechanism for the rapid dissipation of currents.

Syrovatskiĭ [3] was the first to note the possibility of a gradual accumulation of energy in the corona in the field of a current sheet that develops in the neighborhood of a singular line in the potential field, due to disturbances arriving from the photosphere, and Bratenahl and Hirsch [4] demonstrated the rapid decay of current sheets, due to magnetic-field-line reconnection, in their laboratory experiments. The formation of a current sheet in the vicinity of a singular line of the magnetic field has been studied in detail, both theoretically [5, 6] and numerically, in both two-dimensional [7, 8] and three-dimensional [9] MHD simulations. Here, we compare the electrodynamic model of a solar flare [10–12] based on our numerical MHD simulations with new observational data on flares. We discussed the problems arising during numerical simulations of solar flares and their solutions in [13].

Another possible way to form a current sheet is by the injection of a plasma stream into the field of a magnetic arch, with the stream stretching the magnetic-field lines. Such a model was considered by Forbes et al. [14] and Lin [15]. The current sheet in this model is formed by the interaction of the current of a magnetic rope with the magnetic field of the arch. It is assumed that the rope originally develops and is then located above the photosphere, perpendicular to

the magnetic-arch plane. In this case, an equilibrium configuration is created in which the repulsive force on the rope exerted by the current of the mirror image located under the photosphere, $F = \frac{I^2 L}{c^2 r}$, is balanced by the force $\mathbf{I} \times \mathbf{B}_p/c$ acting on the current in the field of the arch. Here, $\mathbf{I}$ is the current in the rope, $\mathbf{B}_p$ the potential field of the arch, r the distance from the rope to the photosphere, L the length of the rope, and c the speed of light. If the repulsive force dominates, equilibrium is disrupted and the rope is accelerated and ejected from the Sun with the formation of a CME. Simultaneously, the arch magnetic-field lines are stretched and a vertical current sheet is formed. The decay of this sheet should give rise to a solar flare. This model [14, 15] accounts for the relationship between CMEs and flares, but does not explain how the current $\mathbf{I}$ forms or why its ejection does not produce strong magnetic disturbances in the photosphere before the flare.

One more possible way in which a flare can develop was suggested by Severnyĭ [16] in view of the detection of accelerated particles in laboratory experiments on powerful pulse discharges [17]. The idea behind this suggestion was the excitation of a field-aligned current in the magnetic loop by some photospheric generator. As the current grows rapidly, the discharge is compressed by its own magnetic field. The compression of the current produces an electric field—$\mathbf{V} \times \mathbf{B}/c$ (where $\mathbf{V}$ is the velocity vector) directed along the axis of the current, which can accelerate particles. This effect was also investigated by Podgorny et al. [18]. The acceleration of charged particles by local electric fields associated with the tearing of the current [19] or due to an abrupt decrease in the conductivity resulting from the action of a prominence on the current filament [20] has also been considered. The idea of a loop current was further developed by Kliem et al. [21]. The possibility of a CME and field-line stretching due to the expansion of a magnetic loop with a field-aligned current was investigated numerically in a MHD approximation for a plasma with $\beta \ll 1$. Kliem et al. [21] assume that the loop expands explosively, as a kink instability develops, and relate the onset of a rapid deformation of the magnetic field with the growth of the current to a critical value at which the torsion of the field lines exceeds 2π. Thus, various models based on a current in a loop can account for some manifestations of flares.

A number of researchers have continued to investigate modifications of the idea of the fast origin of strong magnetic fields over the photosphere, apparently, first put forward by Sokolov [22] in 1981 at the Simferopol seminar on Solar Physics. Possibilities for the expulsion of plasma due to the plasma pressure gradient ∇P have also been considered [23, 24]. The infall of comets into the Sun is also regarded as a possible mechanism for the origin of a large ∇P [25]. The series of studies [23, 26] was dedicated to MHD simulations of the expulsion of a current $\mathbf{I}$ flowing orthogonal to the arch magnetic field by the $\mathbf{I} \times \mathbf{B}/c$ force. The direction of the current $\mathbf{I}$ was assumed to be opposite to the direction specified in Lin's model [15]. The system is not originally in equilibrium, and the current is assumed to grow within a time shorter than the ejection time of the plasma. In the three-dimensional numerical simulations [26], an additional magnetic flux penetrating the arch near the photosphere is also specified to generate the necessary current $\mathbf{I}$. At places where this flux intersects the boundary of the calculation domain, rotation is assumed, the magnetic field lines are twisted and a force-free magnetic rope forms. The results of the MHD computations demonstrate the ejection of a rope anchored in rotating sunspots. As the rope is ejected, the lines of the arched magnetic field are stretched and free magnetic energy is accumulated. For a CME with an energy of $\sim 10^{32}$ erg, it is necessary that this energy be stored in a nonpotential magnetic field over the active region within a time shorter than the duration of the flare, i.e., within $t \sim 10$ s. The question of mechanisms that could provide such a rapid pre-accumulation of energy in the magnetic field, i.e., a rapid increase in the current, is not discussed in [23, 26]. Within the specified 10 s, velocity vortices and magnetic-field disturbances due to the generation of the rope should develop in the photosphere. However, no strong disturbances are observed in the photosphere during flares. In addition, it remains unclear how the assumed unstable equilibrium can originate over an active region under real conditions. The problem of the rapid growth of the current is not considered in the context of Lin's model [15], where the magnetic energy is slowly accumulated in an equilibrium state and, after the loss of stability by the system, is rapidly released high in the corona. The ejection of coronal plasma and the formation of a vertical current sheet were demonstrated in the two-dimensional numerical MHD simulations [27, 28]. However, to specify the initial conditions, a rope in an unstable equilibrium was placed at the neutral point due to the combination of the arch field and the field of the image current.

The above flare models are based on the idea that a current filament forms over the active region. The energy of the ejected current filament acquired due to its interaction with the image current, $W \sim \int_{r_0}^{r} F dr$, where $F = \frac{I^2 L}{c^2 r}$, should exceed the energy of the flare. We assume a filament length of $L = 10^9$ cm and an energy of $W = 10^{32}$ erg to obtain $I \sim \left[W \frac{100}{L \ln(r/r_0)} \right]^{1/2} \sim 10^{12}$ A. The mechanism for

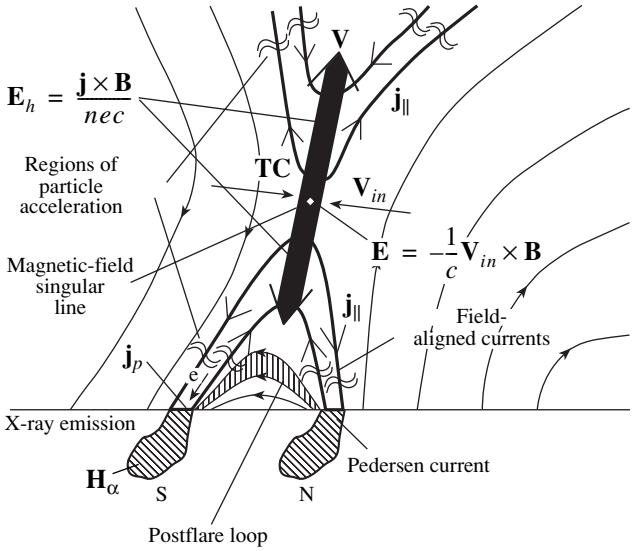

Fig. 1. Electrodynamic model of the flare. The light curves and arrows show the magnetic field lines while the bold curves and arrows show the field-aligned currents.

generating this current remains an unresolved problem. The electrodynamic model of a flare [10–12] is an exception; in this model, the current sheet (CS) is slowly produced in the neighborhood of a singular line by disturbances arriving from the photosphere.

2. ELECTRODYNAMIC MODEL OF A FLARE

The electrodynamic model of the flare [10–12] is based on numerical MHD simulations of current-sheet formation over the active region. It was shown that the current sheet forms before the onset of the flare in the corona, in the neighborhood of the singular line of the magnetic field, due to the focusing of disturbances coming from the photosphere—in particular, fresh magnetic flux whose direction is opposite to that of the old flux of the active region emerges [11]. The current sheet is stable for a long period, and energy is stored in its magnetic field, which is then rapidly released during the solar flare when the current sheet passes into an unstable state. The current sheet is highly stable during its formation due to the presence of a normal magnetic-field component in the sheet (the current sheet is not neutral) and plasma flows along the sheet. This stage is followed by quasi-stationary evolution of the current sheet, during which the total mass of the plasma in the current sheet decreases slowly due to the ejection of a plasma stream accelerated by the magnetic tension from the current sheet. The plasma density is redistributed over the depth of the sheet, so that the plasma density remains virtually constant at the center of the sheet and decreases near its boundary. This evolution changes the current sheet into an unstable state, and the magnetic energy stored in the current-sheet field is rapidly dissipated [29]. Numerical simulations of the transition of a stable sheet stabilized by plasma flows into an unstable state encounters some technical difficulties. An attempt to carry out MHD simulations of the decay of a current sheet in the corona was made in Japan; however, instead of a real, stable current sheet in whose field energy is accumulated, a definitely unstable sheet with zero normal magnetic-field component was specified as the initial state [30].

The basic dissipation mechanism during the explosive decay of a sheet is reconnection, which results in plasma heating in the vicinity of the singular line. The model of a solar flare is shown in Fig. 1. Depending on the initial configuration of the field in the active region and the character of photospheric disturbances in the preflare state, the current sheet can be inclined to the solar surface at various angles. If the current sheet is vertical, as in Fig. 1, the solar flare and CME develop simultaneously, as one explosive process. The plasma flows into the current sheet from both sides with the velocity V_{in}, together with frozen-in magnetic-field lines spreading along the current sheet upward and downward after the field-line reconnection. The $\mathbf{j}\times\mathbf{B}/c$ force (where $\mathbf{j}$ is the current density) accelerates the plasma, and the upward plasma stream ejects the solar material into interplanetary space—a CME develops. The plasma accelerated downward, with shrinking magnetic-field lines, forms postflare loops. The development of a downward plasma stream from the reconnection region during a flare was demonstrated by McKenzie and Hudson [31]. The collection of reconnected field lines over the loop apex should result in the growth of a glowing loop. The upward propagation of the glowing front can create the illusion of an expanding magnetic arch. If the plasma flow accelerated downward becomes super-Alfvénic, a shock can form due to the deceleration of plasma at the loop apex.

Plasma heating due to fast reconnection ensures high temperatures and, therefore, X-ray emission above the loop and at the loop apex. The emergence of hard X-ray radiation from hot plasmoid above the active region in the early stage of a flare was first revealed observationally by the Yohkoh spacecraft [1, 32, 33].

An important property of coronal current sheets is the generation of a Hall electric field, $\mathbf{E}_h = \mathbf{j}\times\mathbf{B}/nec$, within the sheet, whose direction coincides with the plasma flow accelerated along the current sheet. Since the plasma in the coronal magnetic field is highly anisotropic, the Hall field generates electric currents along the magnetic-field lines intersecting the current sheet. The field-aligned currents and their directions are shown by the bold curves and arrows

in the figure. These currents are closed in the chromosphere by Pedersen currents due to the presence of neutral atoms there. The electrons accelerated in the upward, field-aligned current fall onto the chromosphere, giving rise to the glow of flare bands and to hard X-ray emission. The process generating the glow is similar to the mechanism responsible for aurorae [12]. The energy of the X-ray emission due to the electrons falling onto the chromosphere depends on four parameters of the current sheet—the current density and plasma density in the sheet, the normal component of the magnetic field, and the extent of the sheet. Typically, the energies can reach several hundred keV. The falling of fast electrons results in chromospheric evaporation and additional filling of the loop by a plasma stream from the chromosphere [24].

The dissipation of magnetic energy that accompanies the inflow of plasma with frozen-in magnetic field lines should result in the frequently observed the divergence of flare bands. As fresh magnetic-field lines come into the sheet, the footpoints of the flare loop should move relative to each other, together with the field-aligned currents. The streams of accelerated electrons falling onto the solar surface and giving rise to the glow of the bands should move together with the currents. If the sheet is horizontal, the bands can approach each other since field lines from the loop apex come into the sheet in this case [10].

Conditions for the generation of ultrahigh-energy particles—solar cosmic rays—are engendered near the singular line of the magnetic field. In particular, this may be a line of zero magnetic field. The singular line in Fig. 1 is perpendicular to the plane of the sky. The electric field $\mathbf{V_{in}} \times \mathbf{B}/c$ appears as the plasma flows into the current sheet. It is perpendicular to the plane of the sky. Here, $\mathbf{V_{in}}$ is the velocity of the plasma inflow into the sheet, i.e., the reconnection rate, and $\mathbf{B}$ is the magnetic field of the current sheet. Particles (ions and electrons) can be accelerated along the singular line in its vicinity by the electric field—$\mathbf{V_{in}} \times \mathbf{B}/c$. If the maximum inflow velocity is close to the Alfvén speed, the energies of protons can, in principle, exceed hundreds GeV. The particles located farther from the singular line drift in the crossed electric and magnetic fields and cannot reach high energies.

Thus, the energy released during the decay of a current sheet goes into a flare, a CME, and the generation of solar cosmic-ray. Some fraction of the accelerated protons that reach the solar surface produce nuclear reactions accompanied by γ emission. Therefore, the measured duration of the γ emission is determined by the time over which the relativistic protons are generated.

Investigations carried out onboard the RHESSI spacecraft [34, 35] and using neutron monitors [36, 37] and the SSRT radio telescope [38], along with numerical simulations [39, 40], have yielded new evidence for the validity of the electrodynamic model of a flare.

3. PREFLARE MAGNETIC-ENERGY ACCUMULATION

A quantitative analysis of the energy accumulation in the magnetic field of a current sheet needed for a flare was carried out using three-dimensional numerical MHD simulations [39, 40]. No special assumptions about the character of the processes were made. The magnetic field of the active region was approximated by the fields of vertical dipoles placed under the photosphere. The potential magnetic field above the active region was determined in this approximation. The calculated potential magnetic field for four days before the flare was used as the initial magnetic field, and the origin of the current sheet and its evolution associated with the observed variations in the photospheric magnetic field were studied. Three-dimensional MHD computations taking into account dissipation and anisotropy of the thermal conduction were carried out for the preflare state of the Bastille Day flare. It was shown that, before the Bastille Day flare, a current sheet formed over the active region NOAA 9077, and a free energy of $\sim 10^{32}$ erg, sufficient for the flare, was accumulated in its magnetic field.

4. ENERGY OF THE X-RAY EMISSION

X-ray measurements have enabled the acquisition of qualitatively new information concerning the physics of flares. The reason is that data in the visible ($h\nu < 4$ eV) are virtually useless for studying the state of the coronal plasma during the flare, when the electron temperatures are in excess of 1 keV.

Strong plasma heating was recorded by an X-ray telescope onboard the Japanese Yohkoh spacecraft during the flare of January 13, 1992, which was observed at the limb. The X-ray source was located over the apex of an arch near an X-type singular line, where the plasma was heated due to magnetic-energy dissipation [33]. The thermal X-ray emission of this source corresponded to an electron temperature of ~ 10 keV and a density of $\sim 10^{11}$ cm^{-3}.

X-ray observations using the RHESSI spacecraft (Fig. 2) revealed three pronounced centers of X-ray emission associated with a flare [34, 35]. Two spots of hard X-ray emission were recorded at the edge of the solar disk, while the third was located over the limb, i.e., in the corona. In the electrodynamic model, it is there that the radiation source associated with plasma heating due to reconnection in the current

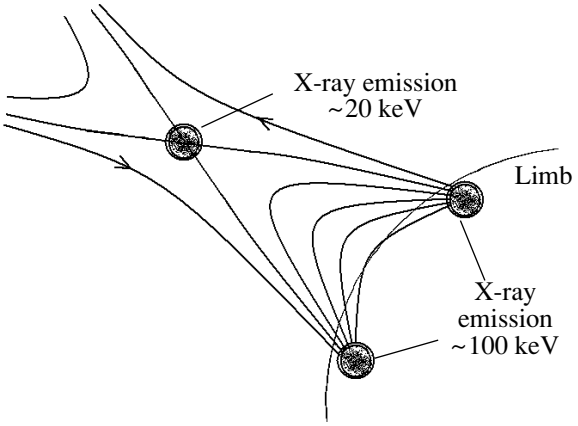

Fig. 2. Location of centers of hard X-ray emission recorded onboard the RHESSI spacecraft during flares near the limb. The map is superposed with magnetic-field lines corresponding to the model of the flare.

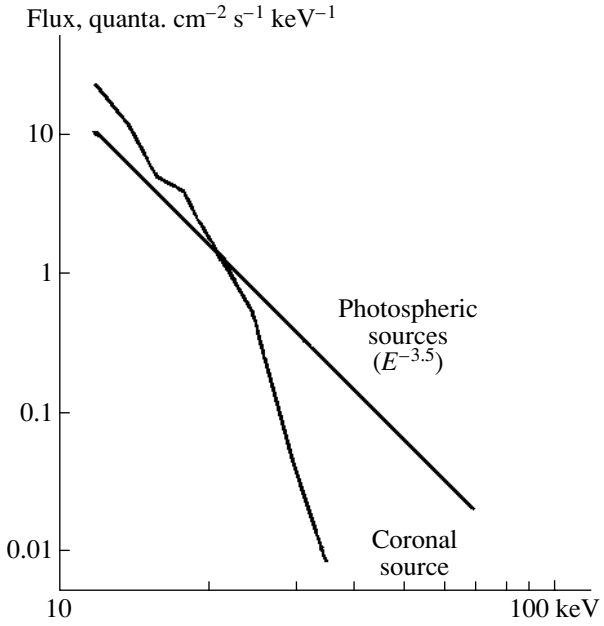

Fig. 3. Sample spectra of hard X-ray emission from a coronal source and from the footpoints of a flare loop (according to RHESSI data).

sheet should be situated. Its emission is thermal and corresponds to a temperature of ~10 keV.

Two other sources were located on either side of the coronal source, at the solar surface, where the footpoints of the magnetic loop should be. The energy emitted by both sources at the solar surface reached ~100 keV. The spectrum was not thermal and had a power-law structure, corresponding to the deceleration of an electron beam in a thick target. Precisely this type of scenario is expected in the electrodynamic model. Beams of fast electrons should be formed due to acceleration in field-aligned currents, so that electrons moving along the magnetic-field lines should fall onto the solar surface. A typical disposition of X-ray sources near the limb during a flare is shown in Fig. 2, based on RHESSI measurements. Sample spectra of the coronal source and the two chromospheric sources are shown in Fig. 3.

The number density $n \sim 10^{11}$ cm^{-3} and electron temperature $T_e \sim 10^3$ eV of the flare-related coronal source determined from the X-ray emission during the flare of January 13, 1992 [33] enable crude estimates of the energy stored in the current-sheet magnetic field up until the onset of the flare and a lower bound for the depth of the current sheet. The pressure balance, $\frac{B^2}{8\pi} = nkT$, implies that the current-sheet magnetic field was then $B \sim 65$ G. The volume occupied by the current-sheet field does not seem to exceed L^3, where L is the size of the active region. For $L \sim 10^{10}$ cm^3, we obtain a magnetic-field energy of $\frac{B^2}{8\pi}L^3 \sim 10^{32}$ erg, which can be released during the flare.

We find from the equation curl$\mathbf{B} = \frac{4\pi \mathbf{j}}{c}$ that $j\delta \sim 100$ A/cm, where δ is the width of the sheet. The maximum possible j is determined by the threshold current velocity corresponding to the development of the ion-acoustic instability, $V_d = \sqrt{\frac{kT_e}{m_i}}$ (m_i is the ion mass). For the measured values of $n = 10^{11}$ cm^{-3} and $T_e = 10^3$ eV, we obtain $j \sim 0.5$ A/cm^2 while the minimum possible δ for fast reconnection is about 200 cm.

5. RELATIONSHIP BETWEEN THE FLARE AND THE CORONAL MASS EJECTION

A number of studies have cast doubt on the relationship between the flare and CME [41], although other authors have taken this point of view to be erroneous [42]. Doubts have stemmed from differences in observational conditions. Flares can be observed under good conditions on the solar disk, while CMEs are best observable near the limb. There is now conclusive evidence that a flare and a CME are manifestations of a single process, at least in the case of major flares. This is indicated by both a statistical analysis of the rates of these phenomena [43] and simultaneous observations of both phenomena at the same site [44].

6. LOCALIZATION OF THE MICROWAVE EMISSION

Comparisons between computed magnetic-field configuration over an active region and the results of radio measurements at 5.2 cm were carried out in [38] for the active region AR 0365, whose field distribution

was not very complex and which gave rise to the flare of May 27, 2003. For the first time, the initial and boundary conditions for the MHD computations were specified using maps of the line-of-sight magnetic field rather than an approximation for the photospheric field using the fields of dipoles or charges. Knowledge of the distribution of the total magnetic-field vector in the photosphere is necessary if we wish to specify the boundary conditions. However, only SOHO MDI data for the line-of-sight magnetic field (http://soi.stanford.edu/magnetic/index5.html) were available to us. For this reason, the magnetic-field components parallel to the photosphere were determined based on a potential field calculated from the line-of-sight magnetic field in the photosphere. This approximation is acceptable since the current sheet is located high above the photosphere and its magnetic field does not substantially affect the photospheric distribution of the field. To this end, the Laplace equation was solved numerically with an oblique derivative as the boundary condition.

The coronal magnetic-field configuration in AR 0365 has several singular lines, near which a current sheet could form due to the focusing of disturbances. We will restrict our consideration here to the singular line near which the most intense current sheet developed and will make a comparison with the most powerful radio pulse recorded on May 27, 2003, by the SSRT radio telescope at 5.2 cm. The greatest increase in the brightness temperature was produced by a flare at 02:53:28.54 UT; the maximum brightness temperature was 1.24×10^7 K. Figure 4b shows the radio-intensity distribution in AR 0365 in the plane of the sky (the plane normal to the line of sight) for 02:53:28.54 UT on May 27, 2003, superposed on the line-of-sight magnetogram. Here, we have used SOHO MDI data (http://soi.stanford.edu/magnetic/index5.html). The heliocentric coordinates of the region of maximum brightness temperature, marked in Fig. 4b with a skew cross, are S6.58 W5.97. The heliocentric coordinates of the singular point of the calculation domain, located where the current sheet is most distinct (at $x = 0.25$, $y = 0.25$, $z = 0.6$ in the calculation domain) at 02:53:28.54, are S7.541 W4.692. The coordinates of the calculation domain were chosen as follows. We used the size of the active region $L_0 = 1.2 \times 10^{10}$ cm as a dimensionless length unit. The Y axis is directed away from the Sun, normal to the photosphere. The X and Z axes lie in the plane of the photosphere, with the X axis pointed west and the Z axis pointing south. For comparison, together with the radio distribution superposed on the magnetogram (Fig. 4b), we present a contour map of the normal magnetic-field component in the plane of the photosphere, calculated in a potential approximation (Fig. 4a). The location of the flare is shown in both maps in Fig. 4 [in Fig. 4b, by the position of the radio-intensity maximum; in Fig. 4a, by the projection onto the photosphere in the direction of the normal at the point ($x = 0.25$, $y = 0.25$, $z = 0.6$)].

The discrepancy in the positions of the flare derived from the radio observations and the MHD simulations does not exceed 1°. This is smaller than the computational errors and the errors in the coordinates on the solar disk. Therefore, the magnetic-field configuration computed in the numerical simulations and the position of the energy-release maximum determined from the radio emission provide evidence for energy dissipation in a current sheet during the flare.

7. SPECTRUM OF SOLAR COSMIC-RAYS

Information about the physics of flares was also obtained independently from the spectra of the relativistic protons [36]. The total duration of the flare proton stream exceeds an hour, while the duration of the γ-ray emission is normally about 10 min. This means that fast protons responsible for nuclear reactions on the Sun accompanied by γ-ray emission are generated near the Sun only during a flare-related explosive energy release. This fast component reaches the Earth along lines of the interplanetary magnetic field, which are in the shape of an Archimedean spiral. Fluxes of protons with energies of up to 10 GeV are recorded at the Earth's surface by the neutron-monitor network. The fast component is recorded at the Earth's orbit about 12 min after the flare. This delay corresponds to the travel time along the Archimedean spiral of the interplanetary magnetic field. Charged particles move in the interplanetary field such that their guiding center remains at a magnetic-field line. Thus, the spectrum of the fast component carries information about the flare acceleration mechanism. The delay of the "slow" solar cosmic-ray flux, which arrives later, is probably determined by diffusive transport and/or the acceleration of protons in a powerful shock at an initial stage of its formation.

In the electrodynamic model, the acceleration mechanism giving rise to the fast component of the relativistic protons is the following. In the case of a reconnection rate of $V_{in} \sim 10^7$ cm/s and a current-sheet magnetic field of $B_{cs} \sim 300$ G, the protons drift toward the sheet in the crossed electric ($E = V_{in}B_{cs}/c$) and nonuniform magnetic fields. The current and magnetic-field distributions for a finite sheet are shown in Fig. 5a. These distributions are plotted in a cross section of the sheet that passes through the neutral line of the magnetic field. The particle

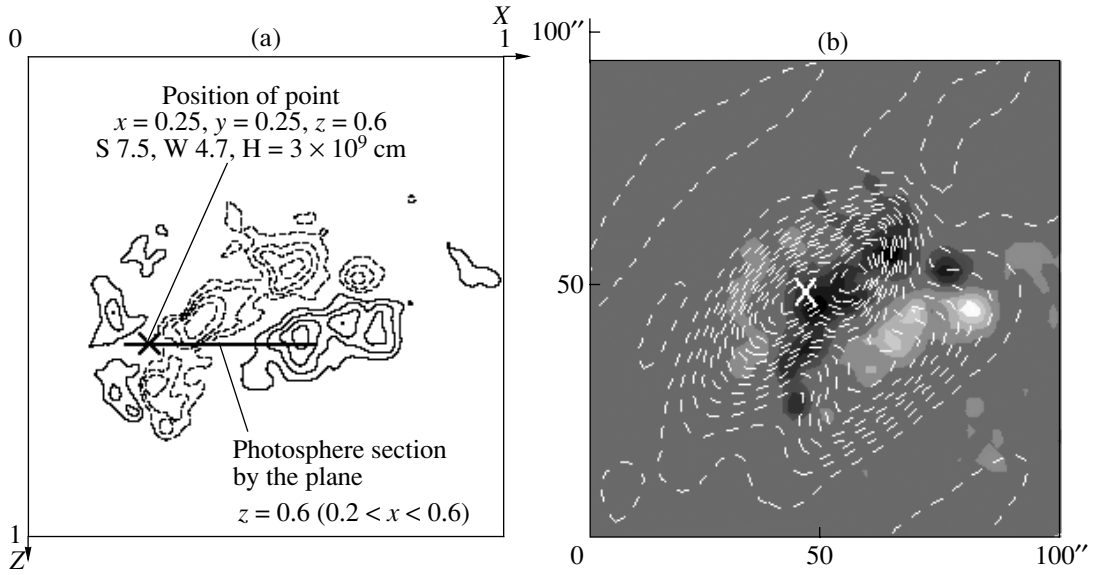

Fig. 4. (a) Contours of the normal magnetic-field component (dashed curves correspond to negative values) at the photospheric boundaries of the calculated domain; the cross marks the position of the point ($x = 0.25$, $y = 0.25$, $z = 0.6$). (b) Distribution of the radio intensity superposed on the magnetogram for the flare of May 27, 2003 at 02:53:28.54 UT; the cross marks the position of the brightness-temperature maximum (whose heliocentric coordinates are S6.58 W5.98).

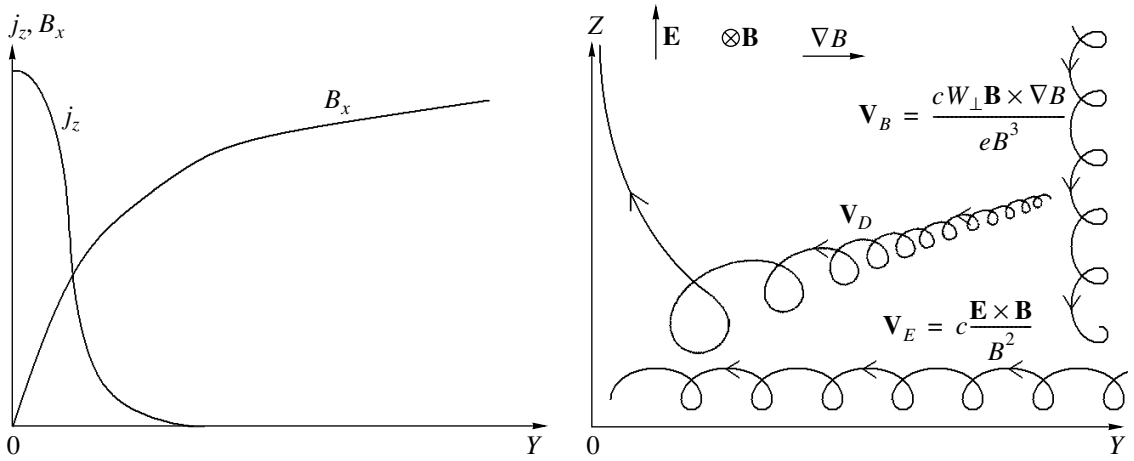

Fig. 5. (a) Distributions of the current density and the magnetic field of the current sheet across the sheet. (b) Drift trajectories of protons in crossed electric and magnetic fields and in a nonuniform magnetic field and the resulting drift in the plane that passes through the neutral line, normal to the sheet.

drifts at the velocity $\mathbf{V} = c\frac{\mathbf{E}\times\mathbf{B}}{B^2}$ in the crossed time-independent fields E and B_{cs}. It simultaneously drifts in the nonuniform magnetic field at the velocity

$$\mathbf{V}_B = \frac{mc(V_\perp^2 + 2V_\parallel^2)}{2eB^3}\mathbf{B}\times\nabla B.$$

These drift trajectories and the trajectory obtained by summing both drifts are shown in Fig. 5b. In such a drift motion toward the sheet $(\mathbf{V}_D\mathbf{E}) < 0$; i.e., the particle, conserving its adiabatic invariant $W_\perp/B$, losses its thermal energy. At a distance of the order of the Larmor radius from the neutral line, the adiabatic law of motion fails, and the particle moving along the electric field begins to rapidly gain energy. Under the action of the magnetic-field component normal to the sheet, a particle that is not moving exactly along the neutral line can be deflected and start drifting in the direction normal to the plane of the sky. Here, the direction of drift in the nonuniform magnetic field in the current sheet coincides with the direction of the electric field so that the particle continues gaining energy (here, $(\mathbf{V}_D\mathbf{E}) > 0$). However, the rate at which such a drifting particle gains energy

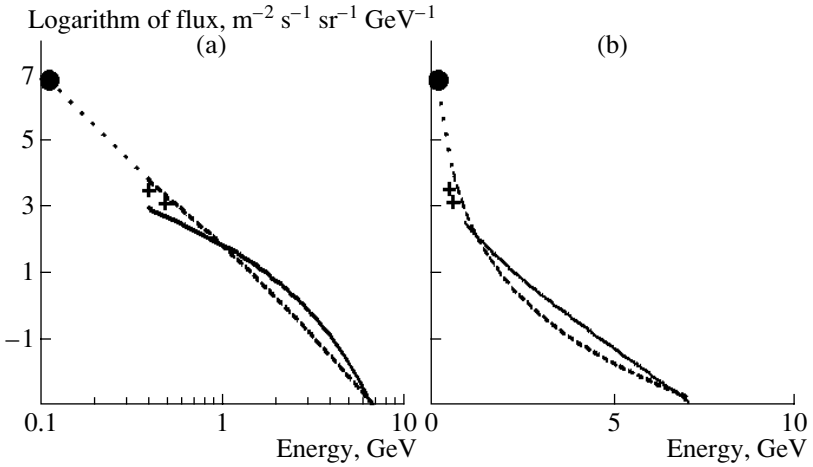

Fig. 6. Spectra of solar cosmic rays for the fast and delayed (dashed curve) components plotted using (a) logarithmic and (b) linear energy scales [36]. (The crosses and the circle represent direct measurements of solar protons on balloons and onboard the GOES 11 spacecraft, respectively.)

is several orders of magnitude lower than the rate of energy gain for motion along the neutral line, and the contribution of the acceleration of the drift motion of relativistic particles proves to be small. The time scale for relativistic protons to gain energy in the electric field in the vicinity of the neutral line is two or three orders of magnitude shorter than the characteristic time for the flare, so that there is no need to take into account the dynamics of changes in the current-sheet configuration when calculating the formation of the proton spectrum.

The spectrum of relativistic protons accompanying a flare was studied using data of the international neutron-monitor network [36, 37]. Depending on the location on the Earth, the neutron monitors detect neutrons produced in the atmosphere by protons that arrived at the Earth at the given time with various energies. A particle with a certain energy that is detected by a monitor comes to the boundary of the magnetosphere at a certain angle. The arrival angle is determined by the motion of the particle in the interplanetary magnetic field. The trajectories of particles with a given energy and a given arrival angle that will be detected by a particular station are calculated for a magnetic field corresponding to the standard model for the magnetosphere. Thus, the entire neutron-monitor network (~30 stations) acts as a multi-channel energy spectrometer. Figures 6a and 6b show the spectra of the fast solar cosmic-ray component and the component that is delayed by 30 min (dashed curve) for the flare of July 14, 2000. A comparison of the spectra plotted on semi–log and log–log scales indicates that the spectrum of the fast component is exponential, while the delayed component has a power-law spectrum. These data indicate that the protons accelerated in the flare itself have an exponential spectrum. Such a spectrum was also obtained in the numerical simulations of acceleration in an electric field directed along a neutral line of the magnetic field [36]. Thus, the exponential spectrum of the fast solar cosmic-ray component provides additional support for the electrodynamic flare model.

8. CONCLUSIONS

(1) Our MHD simulations have demonstrated the formation of a current sheet and the accumulation of energy sufficient for a flare in the sheet magnetic field, above the active region in the preflare state. We specified the initial and boundary conditions using magnetic-field measurements at the photospheric level for the preflare state. We did not introduce any special assumptions about the characters of the processes involved.

(2) RHESSI data have shown that the X-ray emission from the footpoints of a flare loop is produced by beams of falling electrons whose energies substantially exceed the energy of the thermal radiation from the corona generated in the reconnection region.

(3) The exponential spectrum of solar cosmic rays that is formed during the flare suggests that the protons are accelerated in an electric field lying along a singular line of the magnetic field.

(4) The positional coincidence of the current-density maximum obtained from MHD simulations and the maximum of the radio intensity provides direct evidence for a solar-flare mechanism based on the presence of a current sheet in the corona.

(5) The simultaneous formation of a CME, relativistic-proton pulse, and flare provides evidence that a single explosive process is responsible for these phenomena.

All these data are consistent with the scenario for the development of a flare described by the electrodynamic model, based on a slow accumulation of energy above the active region in the field of a current sheet, which is subsequently released in an explosive fashion.

ACKNOWLEDGMENTS

This work was supported by the Russian Foundation for Basic Research (project no. 06-02-16006).

REFERENCES

1. E. Hiei and A. J. Hundhausen, *Magnetodynamic Phenomena in the Solar Atmosphere*, Ed. by Y. Uchida, T. Kosugi, and S. Hudson (Kluwer, Dordrecht, 1996), p. 125.
2. J. Zhang, K. P. Dere, R. A. Howard, et al., Astrophys. J. **599**, 452 (2001).
3. S. I. Syrovatskii, Pis'ma Astron. Zh. **2**, 293 (1976)
4. A. Bratenahl and W. Hirsch, Bull. Am. Phys. Soc. **11**, 580 (1966).
5. B. V. Somov and S. I. Syrovatskii, Tr. Fiz. Inst. im. P.N. Lebedeva, Akad. Nauk SSSR **74**, 14 (1974).
6. B. V. Somov, *Physical Processes in Solar Flares* (Kluwer, Dordrecht, Holland, 1992).
7. K. V. Brushinskii, A. M. Zaborov, and S. I. Syrovatskii, Fiz. Plazmy **6**, 297 (1980) [Sov. J. Plasma Phys. **6**, 114 (1980)].
8. A. I. Podgorny and S. I. Syrovatskii, Fiz. Plazmy **7**, 1055 (1981) [Sov. J. Plasma Phys. **7**, 580 (1981)].
9. A. I. Podgorny, Sol. Phys. **156**, 41 (1995).
10. A. I. Podgorny and I. M. Podgorny, Sol. Phys. **139**, 125 (1992).
11. A. I. Podgorny and I. M. Podgorny, Astron. Zh. **78**, 71 (2001) [Astron. Rep. **45**, 60 (2001)].
12. I. M. Podgorny, A. I. Podgorny, and S. Minami, Astron. Astrophys. Trans. **22**, 585 (2003).
13. A. I. Podgorny and I. M. Podgorny, Zh. Vychisl. Mat. Mat. Fiz. **44**, 1873 (2004).
14. T. G. Forbes, J. M. Malherbe, and E. R. Priest, Sol. Phys. **120**, 258 (1989).
15. J. Lin, Sol. Phys. **219**, 469 (2004).
16. A. B. Severnyi, Izv. Krym. Astrofiz. Obs. **33**, 34 (1965).
17. L. A. Artsimovich et al., At. Energ. **1** (3), 84 (1956).
18. I. M. Podgorny, N. G. Koval'skii, and M. M. Stepanenko, Zh. Eksp. Teor. Fiz. **38**, 1439 (1960) [Sov. Phys. JETP **11**, 1040 (1960)].
19. H. Alfven and G. Arrhenius, *Evolution of the Solar System* (NASA, Washington, 1976).
20. V. V. Zaitsev and V. V. Stepanov, Sol. Phys. **39**, 343 (1992).
21. B. Kliem, V. S. Titov, and T. Torok, Astron. Astrophys. **413**, L23 (2004).
22. V. S. Sokolov, V. S. Slavin, and A. G. Kosovichev, *Year of Solar Maximum* (Akad. Nauk SSSR, Moscow, 1981), p. 211 [in Russian].
23. J. A. Linker, G. Van Hoven, and D. D. Schnack, in *Physics of Magnetic Flux Ropes*, Geophys. Monogr. AGU **58**, 378 (1990).
24. A. I. Podgorny and I. M. Podgorny, Astron. Zh. **76**, 696 (1999) [Astron. Rep. **43**, 608 (1999)].
25. T. V. Losseva, I. B. Kosarev, S. I. Popel, and I. V. Nemtchinov, in *Asteroids, Comets, Meteors,* ESA-SP-500, p. 873 (2002).
26. T. Amari, J. F. Luciami, Z. Mikic, and J. J. Linker, Astrophys. J. **529**, L49 (2000).
27. T. G. Forbes, Geophys, Fluid Dyn. **63**, 15 (1991).
28. Z. Mikic, D. C. Barnes, and D. D. Schnack. Astrophys. J. **328**, 830 (1988).
29. A. I. Podgorny, Sol. Phys. **123**, 285 (1989).
30. T. Yokoyama and K. Shibata, Astrophys. J. **459**, L113 (1998).
31. D. E. McKenzie and H. S. Hudson, Earth, Planets, Space **53**, 577 (2001).
32. S. Masuda, T. Kosugi, H. Hara, et al., Nature **371**, 495 (1994).
33. S. Tsuneta, S. Masuda, T. Kosugi, et al., Astrophys. J. **478**, 787 (1997).
34. S. Krucker, http://sprg.ssl.berkeley.edu/krucker/hessi/clean_real.html.
35. R. P. Lin, S. Krucker, G. J. Hurford, et al., Astrophys. J. **595**, L69 (2003).
36. Yu. V. Balabin, E. V. Vashenyuk, O. V. Mingalev, et al., Astron. Zh. **82**, 940 (2005) [AStron. Rep. **49**, 837 (2005)].
37. I. M. Podgorny, E. V. Vashenyuk, and A. I. Podgorny, in *Proceedings of the Pulkov Seminar on Solar Physics, 2005* (in press).
38. I. M. Podgorny, A. I. Podgorny, and N. S. Meshalkina, in *Proceedings of the Pulkov Seminar on Solar Physics, 2005* (in press).
39. A. I. Podgorny, I. M. Podgorny, and I. A. Bilenko, Izv. Ross. Akad. Nauk, Ser. Fiz. **67**, 406 (2003).
40. I. A. Bilenko, A. I. Podgorny, and I. M. Podgorny, Sol. Phys. **207**, 323 (2002).
41. J. T. Gosling, J. Geophys. Res. **98**, 18937 (1993).
42. M. Dryer, Sol. Phys. **168**, 421 (1996).
43. Chin-Teh Yen, M. D. Ding, and P. F. Chen, in *Proceedings of the IAU 8th Asian-Pacific Regional Meeting, 2002,* Vol. 2, p. 471.
44. J. Zhang, K. P. Dere, R. A. Howard, et al., Astrophys. J. **599**, 452 (2001).

Translated by A. Getling